Adiabatic Control of Quantum Dot Spin in the Voigt Geometry with Optical Pulses

DIONISIS STEFANATOS, NIKOLAOS ILIOPOULOS, VASILIOS KARANIKOLAS, EMMANUEL PASPALAKIS
University of Patras
Materials Science Department
Patras 265 04
GREECE
dionisis@post.harvard.edu, n.iliopoulos@windowslive.com, karanikv@tcd.ie, paspalak@upatras.gr

Abstract: A basic system with important potential applications in quantum technologies is a quantum dot in the Voigt geometry. The spin states of the quantum dot in the Voigt geometry can act as a prototype qubit which can be manipulated by applied optical fields in order to produce the necessary quantum gates. The basic method for spin initialization in a quantum dot in the Voigt geometry is optical pumping. Here, we propose and analyze a new method for the coherent preparation of the quantum dot spin states based on adiabatic control methods. Specifically, we show that the application of two mutually delayed and partially overlapping optical pulses, similar to those used in stimulated Raman adiabatic passage, can lead to initialization of one of the spin states with high fidelity. We also demonstrate that the fidelity of the method may be increased by integrating the quantum dot with a micropillar cavity. Specifically, we show that a preferential Purcell-enhanced decay rate towards the target spin state, in certain cases, increases the fidelity of spin initialization of the adiabatic method. Our results are based on the numerical solution of the relevant density matrix equations for the quantum dot system, either in an isotropic photonic environment or in a micropillar cavity. The calculations presented in this paper are not limited to quantum dots in micropillar cavities. Similar effects can be obtained by other photonic structures as well, as for example, for quantum dots in photonic crystal cavities.

Key–Words: Quantum dot, Optical fields, Voigt geometry, Spin initialization, Adiabatic passage, Purcell effect, Delayed optical pulses

1 Introduction

Electron and hole spin states in semiconductor quantum dots are among the most promising candidates for solid state quantum technologies [1]. Their manipulation can be efficiently achieved by application of optical pulses. This has been verified, for more than a decade, by a series of important experiments for the coherent manipulation, measurement, readout and entanglement of individual spins in quantum dots [2]. Quantum dots can also be efficiently coupled with photonic structures, like microcavities, nanocavities and plasmonic nanostructures, allowing for additional control. An important system that has attracted significant attention in this research area is based on the spin states of a quantum dot in the Voigt geometry (see Fig. 1). A basic problem for the quantum dot electron spin states in the Voigt geometry is the initialization, i.e., the preparation of one of the two electron spin states starting from an equal incoherent mixture, which is the natural initial state of the system. Here, we present and analyze a new method to implement the problem of spin initialization based on adiabatic passage and explore an idea to increase its fidelity.

The basic method for spin initialization in a quantum dot in the Voigt geometry is optical pumping. A resonant optical field couples one of the lower spin states, say state $|1\rangle$, to one of the upper trion states, say state $|4\rangle$. Then, after the excitation to the trion state the population may return to either the coupled spin state $|1\rangle$ and re-excited by the optical field or decay towards state $|2\rangle$ and remain there [3]. If this process lasts several decay times of the trion state, then the population is eventually transferred to state $|2\rangle$ and a single spin state is created from the initial incoherent mixture. The optical pumping process can be accelerated by using a preferential Purcell-accelerated decay rate towards the spin state we desire to create (from state $|4\rangle$ to state $|2\rangle$ in our example). This can be achieved by integration of the quantum dot with micropillar cavities [4, 5], photonic crystal nanocavities [6], metallic nanostructures [7, 8], and even two-dimensional materials [9].

An alternative method for spin initialization has been recently proposed by Paspalakis *et al.* [10],

which has similar and, in some parameters regimes larger, fidelities than optical pumping. This method uses two mutually delayed and partially overlapping optical pulses, similar to those used in stimulated Raman adiabatic passage (STIRAP) [11, 12, 13], for efficient spin initialization in a quantum dot in the Voigt geometry. The duration of this method is fixed by the duration of the applied optical pulses. However, for a fixed pulse duration the fidelity of the method can be altered by different approaches. Here, we show that a preferential Purcell-enhanced decay rate towards the target spin state, in certain cases, increases the fidelity of spin initialization of the adiabatic method. We implement this idea by integrating the quantum dot with a micropillar cavity.

The paper is organized as follows. In the next section, we present the density matrix equations for the time evolution of a quantum dot in the Voigt geometry under the application of two optical pulses. In section 3, we solve numerically the density matrix equations in an isotropic photonic environment and show that efficient spin initialization occurs under the interaction of the quantum dot system with two mutually delayed and partially overlapping optical pulses. The resulted time evolution is explained by a combination of optical pumping in early stages and adiabatic following in the later stages of the dynamics. Then, in section 4 we explore if we can influence the fidelity of the adiabatic spin initialization method presented in section 3 by using enhanced spontaneous decay, via the Purcell effect, towards the target spin state. This is succeeded by placing the quantum dot in an anisotropic photonic environment. Specifically, the quantum dot is placed in a micropillar cavity that enhances the spontaneous decay rate for a specific electric dipole moment direction and does influence the spontaneous decay for electric dipole moments with perpendicular directions [4, 5]. Finally, section 5 concludes our work.

2 Equations for the dynamics of a quantum dot in the Voigt geometry under the application of two optical pulses

We consider a singly-charged self-assembled quantum dot grown along the z-axis. By applying an external magnetic field in the Voigt geometry, along the x-axis, lifts the degeneracy of electron/hole levels by Zeeman splitting. Then, the ground single spin levels are $|1\rangle = |\downarrow_x\rangle$ and $|2\rangle = |\uparrow_x\rangle$ and the two excited trion states are $|3\rangle = |\downarrow_x\uparrow_x\Uparrow_x\rangle$ and $|4\rangle = |\downarrow_x\uparrow_x\Downarrow_x\rangle$. Here, $\Uparrow$ ($\Downarrow$) and $\uparrow$ ($\downarrow$) denote heavy hole and electron spins, respectively. For the level scheme, see

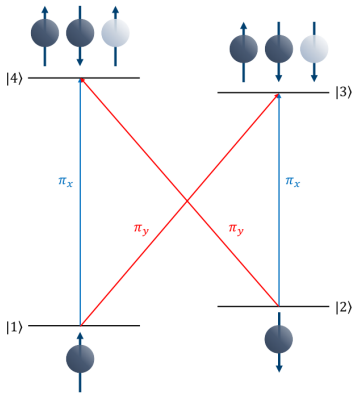

Figure 1: Energy level diagram for a quantum dot in the Voigt geometry. The magnetic field induces the Zeeman splitting in the upper and lower levels.

Fig. 1. Here, the vertical transitions ($|1\rangle \leftrightarrow |4\rangle$ and $|2\rangle \leftrightarrow |3\rangle$) give x-polarized electric dipole moments and the cross transitions ($|1\rangle \leftrightarrow |3\rangle$ and $|2\rangle \leftrightarrow |4\rangle$) give y-polarized electric dipole moments. We take that the quantum dot interacts with two linearly polarized pulsed laser fields with orthogonal polarizations; the field with frequency ω_a (ω_b) has a x-polarized (y-polarized) electric field.

The Hamiltonian that describes the interaction of the optical fields with the quantum dot system, in the dipole and rotating wave approximations, is given by

$$\begin{aligned} H &= \sum_{n=1}^{4} \hbar\omega_n |n\rangle\langle n| - \hbar\Big[\Omega_a(t)e^{-i\omega_a t}|4\rangle\langle 1| \\ &+ \Omega_a(t)e^{-i\omega_a t}|3\rangle\langle 2| + \Omega_b(t)e^{-i\omega_b t}|3\rangle\langle 1| \\ &+ \Omega_b(t)e^{-i\omega_b t}|4\rangle\langle 2| + H.c.\Big]. \end{aligned} \quad (1)$$

Here, $\hbar\omega_n$ with $n = 1 - 4$, is the energy of state $|n\rangle$. Also, $\Omega_a(t)$, $\Omega_b(t)$ are the time-dependent Rabi frequencies defined as $\Omega_a(t) = \Omega f_a(t)$, $\Omega_b(t) = \Omega f_b(t)$, which are assumed real for simplify, where $f_a(t)$, $f_b(t)$ are the dimensionless envelopes of the pulses with frequencies ω_a, ω_b, respectively, and Ω is the maximum value of the Rabi frequencies (taken the same for simplicity for the two pulses). The Hamiltonian of Eq. (1), after a transformation, using the unitary operator $U(t) = e^{-i\sum_{n=1}^{4}\alpha_n|n\rangle\langle n|t}$, where $\alpha_1 = \omega_1$, $\alpha_2 = \omega_a - \omega_b + \omega_1$, $\alpha_3 = \omega_3 + \omega_a - \omega_{41}$, and $\alpha_4 = \omega_a + \omega_1$, gives the interaction Hamiltonian

$$\begin{aligned} H_{eff} &= -\hbar(\omega_a - \omega_b - \omega_{21})|2\rangle\langle 2| \\ &- \hbar(\omega_a - \omega_{41})|3\rangle\langle 3| - \hbar(\omega_a - \omega_{41})|4\rangle\langle 4| \end{aligned}$$

$$
\begin{aligned}
&- \hbar\Big[\Omega_a(t)|4\rangle\langle 1| + \Omega_b(t)|4\rangle\langle 2| \\
&+ \Omega_a(t)e^{-i(\omega_a-\omega_b+\omega_{43})t}|3\rangle\langle 2| \\
&+ \Omega_b(t)e^{i(\omega_a-\omega_b-\omega_{43})t}|3\rangle\langle 1| + H.c.\Big], \quad (2)
\end{aligned}
$$

with $\omega_{nm} = \omega_n - \omega_m$. Also, ω_{21} (ω_{43}) is the Zeeman splitting of the single-electron spin states (heavy-hole spin trion states).

Using the Hamiltonian of Eq. (2) we obtain the equations for the density matrix elements of the system:

$$
\begin{aligned}
\dot\rho_{11}(t) &= \gamma_{41}\rho_{44}(t) + \gamma_{31}\rho_{33}(t) \\
&+ i\Omega_a(t)\rho_{41}(t) - i\Omega_a(t)\rho_{14}(t) \\
&+ i\Omega_b(t)\rho_{31}(t)e^{-i(\omega_a-\omega_b-\omega_{43})t} \\
&- i\Omega_b(t)\rho_{13}(t)e^{i(\omega_a-\omega_b-\omega_{43})t}, \quad (3) \\
\dot\rho_{22}(t) &= \gamma_{32}\rho_{33}(t) + \gamma_{42}\rho_{44}(t) \\
&+ i\Omega_a(t)\rho_{32}(t)e^{i(\omega_a-\omega_b+\omega_{43})t} \\
&- i\Omega_a(t)\rho_{23}(t)e^{-i(\omega_a-\omega_b+\omega_{43})t} \\
&+ i\Omega_b(t)\rho_{42}(t) - i\Omega_b(t)\rho_{24}(t), \quad (4) \\
\dot\rho_{33}(t) &= -(\gamma_{31}+\gamma_{32})\rho_{33}(t) \\
&+ i\Omega_a(t)\rho_{23}(t)e^{-i(\omega_a-\omega_b+\omega_{43})t} \\
&- i\Omega_a(t)\rho_{32}(t)e^{i(\omega_a-\omega_b+\omega_{43})t} \\
&+ i\Omega_b(t)\rho_{13}(t)e^{i(\omega_a-\omega_b-\omega_{43})t} \\
&- i\Omega_b(t)\rho_{31}(t)e^{-i(\omega_a-\omega_b-\omega_{43})t}, \quad (5) \\
\dot\rho_{44}(t) &= -(\gamma_{41}+\gamma_{42})\rho_{44}(t) \\
&+ i\Omega_a(t)\rho_{14}(t) - i\Omega_a(t)\rho_{41}(t) \\
&+ i\Omega_b(t)\rho_{24}(t) - i\Omega_b(t)\rho_{42}(t), \quad (6) \\
\dot\rho_{14}(t) &= -\left[i(\omega_a-\omega_{41}) + \Gamma_{14}\right]\rho_{14}(t) \\
&+ i\Omega_a(t)\left[\rho_{44}(t) - \rho_{11}(t)\right] \\
&+ i\Omega_b(t)\rho_{34}(t)e^{-i(\omega_a-\omega_b-\omega_{43})t} \\
&- i\Omega_b(t)\rho_{12}(t), \quad (7) \\
\dot\rho_{13}(t) &= -\left[i(\omega_a-\omega_{41}) + \Gamma_{13}\right]\rho_{13}(t) \\
&+ i\Omega_b(t)\left[\rho_{33}(t) - \rho_{11}(t)\right]e^{-i(\omega_a-\omega_b-\omega_{43})t} \\
&+ i\Omega_a(t)\rho_{43}(t) \\
&- i\Omega_a(t)\rho_{12}(t)e^{i(\omega_a-\omega_b+\omega_{43})t}, \quad (8) \\
\dot\rho_{12}(t) &= -\left[i(\omega_a-\omega_b-\omega_{21}) + \Gamma_{12}\right]\rho_{12}(t) \\
&+ i\Omega_a(t)\rho_{42}(t) \\
&+ i\Omega_b(t)\rho_{32}(t)e^{-i(\omega_a-\omega_b-\omega_{43})t} \\
&- i\Omega_a(t)\rho_{13}(t)e^{-i(\omega_a-\omega_b+\omega_{43})t} \\
&- i\Omega_b(t)\rho_{14}(t), \quad (9) \\
\dot\rho_{34}(t) &= -\Gamma_{34}\rho_{34}(t) \\
&+ i\Omega_a(t)\rho_{24}(t)e^{-i(\omega_a-\omega_b+\omega_{43})t} \\
&+ i\Omega_b(t)\rho_{14}(t)e^{i(\omega_a-\omega_b-\omega_{43})t} \\
&- i\Omega_a(t)\rho_{31}(t) - i\Omega_b(t)\rho_{32}(t), \quad (10) \\
\dot\rho_{24}(t) &= -\left[i(\omega_b-\omega_{42}) + \Gamma_{24}\right]\rho_{24}(t) \\
&+ i\Omega_a(t)\rho_{34}(t)e^{i(\omega_a-\omega_b+\omega_{43})t} \\
&+ i\Omega_b(t)\left[\rho_{44}(t) - \rho_{22}(t)\right] \\
&- i\Omega_a(t)\rho_{21}(t), \quad (11) \\
\dot\rho_{23}(t) &= -\left[i(\omega_b-\omega_{42}) + \Gamma_{23}\right]\rho_{23}(t) \\
&+ i\Omega_a(t)\left[\rho_{33}(t) - \rho_{22}(t)\right]e^{i(\omega_a-\omega_b+\omega_{43})t} \\
&+ i\Omega_b(t)\rho_{43}(t) \\
&- i\Omega_b(t)\rho_{21}(t)e^{-i(\omega_a-\omega_b-\omega_{43})t}, \quad (12)
\end{aligned}
$$

with $\sum_n \rho_{nn}(t) = 1$, $\rho_{nm}(t) = \rho^*_{mn}(t)$. Here, γ_{nm} are the population decay rates and $\Gamma_{nm} = \Gamma_{mn}$ the coherence decay rates, which are given by $\Gamma_{14} = \Gamma_{24} = (\gamma_{41}+\gamma_{42})/2$, $\Gamma_{13} = \Gamma_{23} = (\gamma_{31}+\gamma_{32})/2$, $\Gamma_{34} = (\gamma_{31}+\gamma_{32}+\gamma_{41}+\gamma_{42})/2$, and $\Gamma_{12} = 0$.

Here, we will assume that the two laser pulses are at single photon resonance with specific transitions, such as $\omega_a = \omega_{41}$ and $\omega_b = \omega_{42}$. The dimensionless pulse envelopes are taken

$$
\begin{aligned}
f_a(t) &= e^{-(t-t_f/2-\eta)^2/t_p^2}, \quad (13) \\
f_b(t) &= e^{-(t-t_f/2+\eta)^2/t_p^2}, \quad (14)
\end{aligned}
$$

where η is the pulse delay, $t_f/2$ determines the center of the laser pulses for $\eta = 0$, and t_p determines the width of the pulses.

3 The idea of adiabatic spin initialization with delayed optical pulses

In Fig. 2 we present calculations for the evolution of the population of the four quantum states under the application of the optical fields. Initially, we assume that the quantum dot is in an isotropic environment (e.g. free space or a homogeneous dielectric) such that the excited trion states decay to the ground spin states with the same population decay rate Γ. Therefore, in accordance to previous work [3, 10, 14], we take $\gamma_{31} = \gamma_{32} = \gamma_{41} = \gamma_{42} = \Gamma$. For this figure, and for the rest of the article the parameters of the quantum dot are taken $\hbar\Gamma = 1.2$ μeV, $\hbar\omega_{21} = 0.124$ meV, $\hbar\omega_{43} = 0.078$ meV (the Zeeman splittings correspond to magnetic field ~ 8 T), typical for InAs quantum dots [3, 14]. The parameters for the laser fields are taken $\Omega = 2\pi$ ns^{-1}, $t_p = t_f/6$ ns, $\eta = t_f/8$, unless stated otherwise. In all the calculations in this work the quantum dot system starts from an initial incoherent mixture of the two electron-spin states, so $\rho_{11}(0) = 1/2$, $\rho_{22}(0) = 1/2$, $\rho_{33}(0) = \rho_{44}(0) = 0$, and $\rho_{nm}(0) = 0$ with $n \neq m$.

In Fig. 2 we present the time evolution of the population in the different states for the system interacting with Gaussian pulses of Eqs. (13) and (14). In the

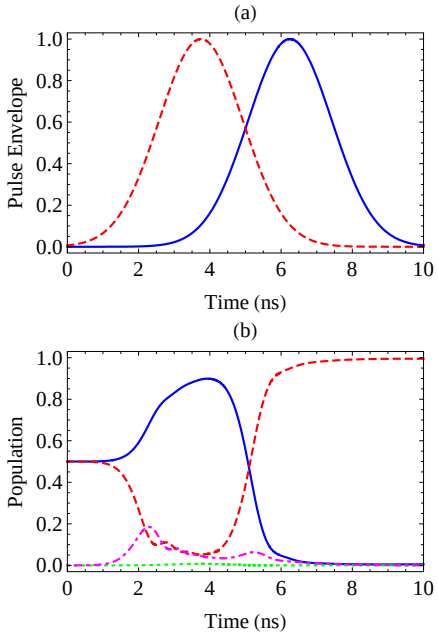

Figure 2: (a) The pulse envelopes from Eqs. (13) and (14) with frequency ω_a (solid curve) and with frequency ω_b (dashed curve). (b) The time evolution of the population, $\rho_{nn}(t)$ with $n = 1 - 4$, of states $|1\rangle$ (solid curve), $|2\rangle$ (dashed curve), $|3\rangle$ (dotted curve) and $|4\rangle$ (dash-dotted curve) for Gaussian pulses of Eqs. (13) and (14) with $t_f = 10$ ns.

presented case the pulse with frequency ω_b precedes that with frequency ω_a in both switch on and switch off, see Fig. 2(a). The dynamics of the population in Fig. 2(b) shows that the population is partially transferred for short times to state $|1\rangle$, but at later times it is efficiently, almost completely, transferred to state $|2\rangle$. The final population of spin state $|2\rangle$ is 0.995211. We note that if we reverse the time order of the two pulses, then the spin state $|1\rangle$ will be created. Also, if we change the time-dependent Rabi frequencies so that the two optical pulses are switched on in the same manner as in Fig. 2(a) and switched off simultaneously, any coherent superposition of the spin states $|1\rangle$ and $|2\rangle$ may be created [10].

Let us explain the behavior of the system. As the two pulses are applied at single-photon resonance and $\omega_{21} \pm \omega_{43} > \Omega$ we can assume that the terms with $e^{\pm i(\omega_a - \omega_b \pm \omega_{43})t}$ can be omitted from the Hamiltonian of Eq. (2), so effectively we get a three-level Λ-type system for states $|1\rangle$, $|2\rangle$ and $|4\rangle$, while state $|3\rangle$ is practically not coupled to the optical pulses. Then, the effective Hamiltonian for this reduced Λ-type system is

$$\begin{aligned} H_\Lambda &= -\hbar(\omega_a - \omega_{41})|3\rangle\langle 3| - \hbar(\omega_a - \omega_{41})|4\rangle\langle 4| \\ &- \hbar\Big[\Omega f_a(t)|4\rangle\langle 1| \\ &+ \Omega f_b(t)|4\rangle\langle 2| + H.c.\Big]. \end{aligned} \tag{15}$$

An important property of Eq. (15) is the existence of an eigenstate with a zero eigenvalue, the so-called dark state, which has the form:

$$\begin{aligned} |\psi_{Dark}(t)\rangle &= \frac{f_b(t)}{\sqrt{f_a^2(t) + f_b^2(t)}}|1\rangle \\ &- \frac{f_a(t)}{\sqrt{f_a^2(t) + f_b^2(t)}}|2\rangle . \end{aligned} \tag{16}$$

The evolution of the quantum dot spin presented above can be understood by splitting the dynamics in two parts. As the initial state of the system is an incoherent mixture of the two spin states, the population is initially divided between the two lower states $|1\rangle$ and $|2\rangle$ and no initial coherence exists. At early times only one laser pulse is applied (in our case the pulse with frequency ω_b). Then, at this time period, the uncoupled lower state, state $|1\rangle$, gains population via optical pumping [3]. Then, the second field is switched on, and the system can be described by the Hamiltonian of Eq. (15) and, if the interaction is adiabatic, the system follows the evolution of the dark state, Eq. (16). In that time period the population can be completely transferred to state $|2\rangle$. The later part of the dynamics, i.e., after the second field is switched on, is similar to STIRAP [11, 12, 13].

4 Increasing the fidelity of spin initialization using the Purcell effect

We will now explore if we can influence the fidelity of the adiabatic spin initialization method with delayed optical pulses by using enhanced spontaneous decay, via the Purcell effect. To this end we assume that the quantum dot is placed in a micropillar cavity, see Fig. 3, that enhances the spontaneous decay rate for a y-polarized electric dipole moment but does influence the spontaneous decay for a x-polarized electric dipole moment [4, 5]. In this case spontaneous emission rates are given by

$$\gamma_{41} = \gamma_{32} = \Gamma, \quad \gamma_{42} = \gamma_{31} = F_p\Gamma , \tag{17}$$

where F_p is the Purcell factor for the enhancement of the spontaneous emission by the micropillar cavity, with $F_p > 1$.

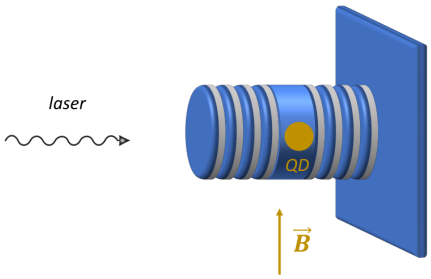

Figure 3: A quantum dot in the Voigt geometry placed in a micropillar cavity.

In Fig. 4 we present the time evolution of the population in the different states for the system interacting with Gaussian pulses of Eqs. (13) and (14) in the case that the quantum dot system in placed in a micropillar cavity for three different cases of the Purcell factor F_p, $F_p = 3, 6, 9$ for (a), (b), (c), respectively. The dynamics of the population in Fig. 4 is similar to that of Fig. 2. However, in every case, the final population of spin state $|2\rangle$ increases in comparison to the result of Fig. 2 and becomes 0.999632 for $F_p = 3$, 0.999373 for $F_p = 6$ and 0.998793 for $F_p = 9$, so in every case presented in Fig. 4 the fidelity of spin initialization is larger than in the case of the quantum dot without the cavity [compare with the results shown in Fig. 2(b)]. The increase of the fidelity is important for quantum technologies applications, as there almost unity fidelity is desired.

Performing additional calculations, we have found that larger initialization fidelities are obtained up to Purcell factors $F_p \approx 17.5$ for the quantum dot with the microrpillar cavity than without the cavity, for the used parameters. For larger values of F_p the fidelities for the quantum dot with the micropillar cavity are smaller than without the micropillar cavity and also the fidelities gradually decrease with the increase of the Purcell factor. This is shown in Fig. 5, where the final population of the target state $|2\rangle$ is shown as a function of F_p for different values of Ω. The same behavior occurs for different Ω, as it can be seen from Fig. 5. In every case the maxima of the fidelities are obtained for $3.2 < F_p < 3.7$. Also, the maximum value of F_p that gives larger initialization fidelities for the quantum dot with the microrpillar cavity than without the cavity varies with the actual value of Ω. Note that the Purcell factors needed for the enhancement of fidelity are within current experimental capabilities [15].

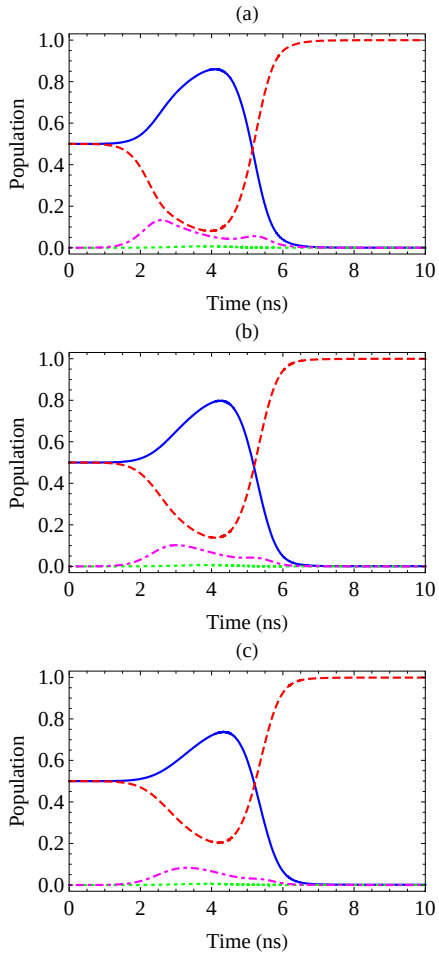

Figure 4: The time evolution of the population, $\rho_{nn}(t)$ with $n = 1 - 4$, of states $|1\rangle$ (solid curve), $|2\rangle$ (dashed curve), $|3\rangle$ (dotted curve) and $|4\rangle$ (dash-dotted curve) for Gaussian pulses of Eqs. (13) and (14) with $t_f = 10$ ns for the quantum dot in the micropillar cavity. In (a) $F_p = 3$, in (b) $F_p = 6$, and in (c) $F_p = 9$.

5 Conclusion

In this work, we presented an alternative method to optical pumping for spin initialization in a quantum dot in the Voigt geometry. The method uses two mutually delayed and partially overlapping optical pulses, which lead to an adiabatic evolution of the quantum system, for the efficient spin initialization in a quantum dot in the Voigt geometry. We also analyzed the potential of increasing the fidelity of the method by a preferential Purcell-enhanced decay rate towards the target spin state. We showed that the fidelity of

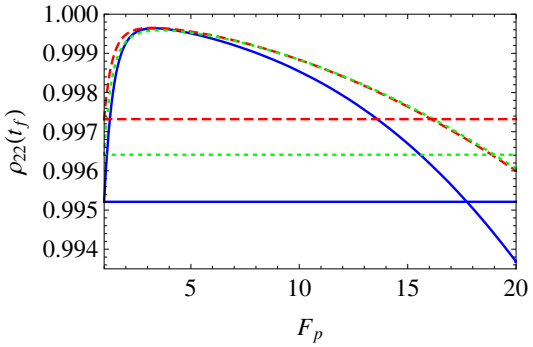

Figure 5: The population of state $|2\rangle$ at $t = t_f$, $\rho_{22}(t_f)$, as a function of F_p for different values of Ω, namely $\Omega = 2\pi$ ns^{-1} (solid curve), $\Omega = 4\pi$ ns^{-1} (dashed curve), and $\Omega = 6\pi$ ns^{-1} (dotted curve) with $t_f = 10$ ns for the quantum dot in the micropillar cavity. The horizontal lines indicate the value of $\rho_{22}(t_f)$ without the micropillar cavity for the different values of Ω.

spin initialization of the quantum dot may increase by integrating the quantum dot with a micropillar cavity. Before closing, we note that the calculations presented above are not limited to quantum dots in micropillar cavities. Similar effects can be obtained by other photonic structures as well, as for example, for quantum dots in photonic crystal cavities [16]. The methods presented in this work are particularly important in quantum technologies applications, namely in the preparation of qubits, and in nanophotonics. For future research, we intend to combine the presented methodologies with shortcuts to adiabaticity methods [17], as well as, optimal control methods [18] for increasing the fidelity of the initialization process for shorter electromagnetic pulses.

Acknowledgements: The research is implemented through the Operational Program "Human Resources Development, Education and Lifelong Learning" and is co-financed by the European Union (European Social Fund) and Greek national funds (project EΔBM34, code MIS 5005825). E.P. would like to thank Profs. Fernando Carreño, Sophia E. Economou, and Ioannis Thanopulos for useful discussions and help.

References:

[1] R. J. Warburton, Single spins in self-assembled quantum dots, *Nat. Mater.* 12, 2013, pp. 483–493.

[2] W. B. Gao, A. Imamoglu, H. Bernien, and R. Hanson, Coherent manipulation, measurement and entanglement of individual solid-state spins using optical fields, *Nat. Photon.* 9, 2015, pp. 363–373.

[3] C. Emary, X. Xu, D. G. Steel, S. Saikin, and L. J. Sham, Fast initialization of the spin state of an electron in a quantum dot in the Voigt configuration, *Phys. Rev. Lett.* 98, 2007, art. no. 047401.

[4] V. Loo, L. Lanco, O. Krebs, P. Senellart, and P. Voisin, Single-shot initialization of electron spin in a quantum dot using a short optical pulse, *Phys. Rev. B* 83, 2011, art. no. 033301.

[5] P. Kumar and T. Nakajima, Fast and high-fidelity optical initialization of spin state of an electron in a semiconductor quantum dot using light-hole-trion states, *Opt. Commun.* 370, 2016, pp. 103-109.

[6] A. Majumdar, P. Kaer, M. Bajcsy, E. D. Kim, K. G. Lagoudakis, A. Rundquist, and J. Vuckovic, Proposed coupling of an electron spin in a semiconductor quantum dot to a nanosize optical cavity, *Phys. Rev. Lett.* 111, 2013, art. no. 027402.

[7] M. A. Antón, F. Carreño, S. Melle, O. G. Calderón, E. Cabrera-Granado, and M. R. Singh, Optical pumping of a single hole spin in a p-doped quantum dot coupled to a metallic nanoparticle, *Phys. Rev. B* 87, 2013, art. no. 195303.

[8] F. Carreño, F. Arrieta-Yáñez, and M. A. Antón, Spin initialization of a p-doped quantum dot coupled to a bowtie nanoantenna, *Opt. Commun.* 343, 2015, pp. 97–106.

[9] D. Stefanatos, V. Karanikolas, N. Iliopoulos, and E. Paspalakis, Fast spin initialization of a quantum dot in the Voigt configuration coupled to a graphene layer, *Physica E* 117, 2020, 113810.

[10] E. Paspalakis, S. E. Economou, and F. Carreño, Adiabatically preparing quantum dot spin states in the Voigt geometry, *J. Appl. Phys.* 125, 2019, art. no. 024305.

[11] P. Kral, I. Thanopulos, and M. Shapiro, Coherently controlled adiabatic passage, *Rev. Mod. Phys.* 79, 2007, pp. 53-77.

[12] B. W. Shore, Picturing stimulated Raman adiabatic passage: a STIRAP tutorial, *Adv. Opt. Photon.* 9, 2017, pp. 563-719.

[13] N. V. Vitanov, A. A. Rangelov, B. W. Shore, and K. Bergmann, Stimulated Raman adiabatic passage in physics, chemistry, and beyond, *Rev. Mod. Phys.* 89, 2017, 015006.

[14] S. E. Economou and T. L. Reinecke, Theory of fast optical spin rotation in a quantum dot based on geometric phases and trapped states, *Phys. Rev. Lett.* 99, 2007, 217401.

[15] H. Wang *et al.*, Towards optimal single-photon sources from polarized microcavities, *Nature Photonics* 13, 2019, pp. 770-775

[16] F. Liu *et al.*, High Purcell factor generation of coherent on-chip single photons, *Nature Nanotechnology* 13, 2018, pp. 835-840.

[17] D. Guéry-Odelin, A. Ruschhaupt, A. Kiely, E. Torrontegui, S. Martínez-Garaot, and J. G. Muga, Shortcuts to adiabaticity: Concepts, methods, and applications, *Rev. Mod. Phys.* 91, 2019, art. no. 045001.

[18] D. Stefanatos and E. Paspalakis, Efficient generation of the triplet Bell state between coupled spins using transitionless quantum driving and optimal control, *Phys. Rev. A* 99, 2019, art. no. 022327.